第 35 卷 第 4 期
2018 年 12 月

原 子 核 物 理 评 论
Nuclear Physics Review

Vol. 35, No. 4
Dec., 2018

Article ID: 1007-4627(2018) 04-0511-07

Nuclear Shape Phase Crossover in $A\sim$130 Mass Region in the *SD*-pair Shell Model

DING Xiaoxue[1], LUO Yanan[2], HE Bingcheng[2], PAN Feng[1,3], ZHANG Yu[1], LI Bo[4], J. P. Draayer[3]

(*1. Department of Physics, Liaoning Normal University, Dalian 116029, Liaoning, China;*
2. School of Physics, Nankai University, Tianjin 300071, China;
3. Department of Physics and Astronomy, Louisiana State University, Baton Rouge, Louisiana 70803-4001, USA;
4. Department of Physics, Anshan Normal University, Anshan 114007, Liaoning, China)

Abstract: The *SD*-pair shell model is applied to analyze the evolution of low-lying states of even-even nuclei in $A\sim 130$ mass region. In the model, the pairing and the quadrupole-quadrupole interactions are taken into account. The results show that there are clear signatures of the crossover from vibrational to rotational or from vibrational to the γ-soft shape phase.

Key words: *SD*-pair shell model; shape phase crossover; energy ratio; electromagnetic transition

CLC number: O571.6 **Document code:** A **DOI:** 10.11804/NuclPhysRev.35.04.511

1 Introduction

As is well known, nuclei as a complex system have been found to be with various geometric shapes. A lot of theoretical investigations on the shape phase transitions in nuclei were carried out[1–20] mainly within the interacting boson model (IBM).

Recently, there have been many works on nuclear shape phase transitions and their critical point symmetries in the framework of shell model based on the *SD*-pair shell model[21–23], relativistic mean field approach[24], and density functional approach[25]. The investigations on nuclear shape phase transition for identical nucleon system have also been carried out with fermionic degrees of freedom in Refs. [15, 26–30]. The tremendous success of IBM [1], suggests that *S* and *D* pairs play a dominant role in the spectroscopy of low-lying modes[31–33]. Therefore, one normally truncates the full shell-model space to the collective *SD*-pair subspace in the NPSM. The latter is called the *SD*-pair shell model(SDPSM)[34–36]. The advantages of the NPSM are that it accommodates various truncation, ranging from the truncation to only the *S* subspace, the *S*-*D* subspace, up to the full shell model space, and that it is flexible enough to include the broken pair approximation[37], the pseudo $SU(2)$ or the favored pair model[38] and the fermion dynamical symmetry model[39] as its special cases.

Since the model space is also built up from *SD* pairs, it is interesting to see if the nuclear shape phase transitional patterns produced from IBM[1] can be produced in the SDPSM, which is the main objective of this work.

2 Model overview

The collective pair $A^{r^\dagger}_\mu$ of proton or neutron with angular momentum $r(r=0,2)$ and projection μ is built from many non-collective pairs $A^r_\mu(ab)$ with the single-particle orbits a and b, which defined as

$$A^{r^\dagger}_\mu=\sum_{ab}y(abr)A^{r^\dagger}_\mu(ab)=\sum_{ab}y(abr)(C^\dagger_a\times C^\dagger_b)^r_\mu, \quad (1)$$

where $y(abr)$ are the structure coefficients of the multi-pair and determined properly by the composition, satisfying the symmetry

$$y(abr)=-\theta(abr)y(abr), \quad \theta(abr)=(-)^{a+b+r}. \quad (2)$$

In this work, the *S*-pair structure coefficients are determined as $y(aa0)=\sqrt{2j_a+1}\frac{v_a}{u_a}$, where v_a and u_a are the occupied and unoccupied amplitudes for orbit a obtained by solving the associated BCS equation.

Received date: 11 Sep. 2018; **Revised date:** 13 Nov. 2018

Foundation item: National Natural Science Foundation of China (11675071, 11747318, 11475091, 11875171); U. S. National Science Foundation (OIA-1738287, ACI -1713690); U. S. Department of Energy (DE-SC0005248); China-U. S. Theory Institute for Physics with Exotic Nuclei (CUSTIPEN) (DE-SC0009971); LSU–LNNU Joint Research Program (9961); Research Start-up Fund of Anshan Normal University (2018b03)

Biography: DING Xiaoxue(1987–), femal, Anshan, Liaoning Province, Ph.D., working on nuclear physics;
E-mail: wojiaodingxiaoxue@126.com.

In order to construct spherical tensors, we introduce the time reversed operator instead of the annihilation operator. The time reversed pair operator $\tilde{A}^r_\mu$ with angular momentum r is

$$\tilde{A}^r_\mu = \sum_{ab} y(abr)\tilde{A}^r_\mu(ab) = -\sum_{ab} y(abr)(\tilde{C}_a \times \tilde{C}_b)^r_\mu, \quad (3)$$

where $\tilde{C}_{a\alpha} = (-)^{a-\alpha}C_{a-\alpha}$, and $C_{a\alpha}$ is the annihilation operator.

For an even-even system, we choose $n = 2N$ valence nucleons coupled N collective pairs with angular momenta $r_1, r_2, \cdots, r_N$ as our model basis. Obviously,

$$\begin{aligned} &A^{J^\dagger_N}_{M_N}(r_i, J_i) = A^{J^\dagger_N}_{M_N}(r_1 r_2 \cdots r_N,\ J_1 J_2 \cdots J_N) \\ =&(\cdots((A^{r_1^\dagger} \times A^{r_2^\dagger})^{J_2} \times A^{r_3^\dagger})^{J_3} \times \cdots \times A^{r_N^\dagger})^{J_N}_{M_N} \end{aligned} \quad (4)$$

with the convention $r_1 \geqslant r_2 \geqslant \cdots \geqslant r_N$. Here J_N is the total angular momentum with its projection of M_N. We use $(r_1 r_2 \cdots r_N)$ and $(J_1 J_2 \cdots J_N)$ with $J_1 = r_1$ for the angular momenta of the pairs involved and coupled ones, respectively, for the N-pair operator.

It's worth noting that there are several possible values for each of the intermediate, but the largest possible intermediate angular momentum values J_i is taken in this paper to solve the complete basis issue. The same r_i, J_N, M_N in those functions, while different J_i , $i = 2, \cdots, N-1$ just form an overcomplete basis [34]. For example, five D pairs can be denoted as the followinng form,

$$\begin{aligned} &|(D^\dagger)^5(S^\dagger)^{N-5}, J_1 J_2 J_3 J_4 J_5\rangle, J_1 J_2 J_3 J_4 J_5 \\ =&24420, 24442, 24642, 24653, 24654, 24664, \\ &24665, 24666, 24686, 24687, 24688, 246810. \end{aligned} \quad (5)$$

In the calculation, the multipair basis states[35, 40] with both valence neutrons and valence protons is used with

$$|(D^\dagger_\nu)^{n_\nu}(S^\dagger_\nu)^{N_\nu - n_\nu}(D^\dagger_\pi)^{n_\pi}(S^\dagger_\pi)^{N_\pi - n_\pi}; JM\rangle.$$

Here

$$\begin{aligned} &|(D^\dagger_\nu)^{n_\nu}(D^\dagger_\pi)^{n_\pi}; JM\rangle = \\ &\sum_{M_\nu M_\pi} C^{JM}_{J_\nu M_\nu, J_\pi M_\pi} |J_\nu M_\nu\rangle |J_\pi M_\pi\rangle, \end{aligned} \quad (6)$$

in which N_ν (N_π) is the number of pairs for valence neutrons (protons) with appropriate angular momentum J_ν (J_π). By coupling the neutron and proton states to the states, the total angular momentum is denoted by J with its projection of M.

The matrix elements in the multi-pair basis can be expressed in terms of the overlap of the multi-pair states, and the latter can be calculated recursively by[34]

$$\begin{aligned} &\langle 0|A^{J_N}_{M_N}(s_i, J'_i)A^{J_N}_{M_N}(r_i, J_i)^\dagger|0\rangle \\ =&\langle s_1 s_2 \cdots s_N;\ J'_1 \cdots J'_{N-1} J_N | r_1 r_2 \cdots r_N;\ J_1 \cdots J_{N-1} J_N\rangle \\ =&(\hat{J}'_{N-1}/\hat{J}_N)(-)^{J_N + s_N - J'_{N-1}} \sum_{k=N}^{1} \sum_{L_{k-1}\cdots L_{N-1}} H_N(s_N)\cdots H_{k+1}(s_N)\times \\ &\Big[\psi_k \delta_{s_N, r_K}\delta_{L_{k-1}, J_{k-1}}\langle s_1 s_2 \cdots s_{N-1};\ J'_1 \cdots J'_{N-1}|r_1 \cdots r_{k-1}, r_{k+1}\cdots r_N;\ J_1 \cdots J_{k-1} L_k \cdots L_{N-1}\rangle + \\ &\sum_{i=k-1}^{1} \sum_{r'_i L_i \cdots L_{k-2}} \langle s_1 s_2 \cdots s_{N-1};\ J'_1 \cdots J'_{N-1}|r_1 \cdots r'_i \cdots r_{k-1}, r_{k+1}\cdots r_N;\ J_1 \cdots J_{i-1} L_i \cdots L_{N-1}\rangle\Big], \end{aligned} \quad (7)$$

where $\hat{J} = \sqrt{2J+1}$, $H_k(s)$ are Racah coefficients which induced by various re-coupling procedures. ψ_k is a constant coming from the annihilation of the pair $A^{r_k\dagger}$ by A^{s_N}, and thus depends on the structure of these two pairs, while r'_i represents a new collective pair $B^{r'_i\dagger}$ resulting from a double-process. In this work, the calculation of matrix elements is based on the right to left convention. Firstly, the pair A^{s_N} transforms the pair $A^{r_k\dagger}$ into a particle-hole pair $\mathcal{P}^t$ with angular momentum t, which then propagates forward, crosses over the pairs $r_{k-1}, \cdots, r_{i+1}$, and finally transforms the pair $A^{r_i\dagger}$ into the new pair $B^{r'_i\dagger} = \left[A^{r_i\dagger}, \mathcal{P}^t\right]^{r'_i}$, with a new distribution function $y'(a_k a_i r'_i)$ depending on the structure of all the three pairs $A^{r_k\dagger}$, $A^{r_i\dagger}$ and $A^{s_N\dagger}$, and the intermediate quantum numbers $L_i \ldots L_{k-2} L_{k-1}$. The right hand side of Eq. (7) is a linear combination of the overlaps for N-1 pairs. Thus, the overlap can be calculated recursively.

The Hamiltonian [41] is chosen as

$$\begin{aligned} H &= \sum_{\sigma=\pi,\ \nu} H_\sigma + H_{\pi\nu}, \\ H_\sigma &= \sum_a \epsilon_{\sigma a} n_{\sigma a} - G_\sigma S^\dagger_\sigma S_\sigma - \kappa_\sigma Q^2_\sigma \cdot Q^2_\sigma, \\ H_{\pi\nu} &= -\kappa_{\pi\nu} Q^2_\pi \cdot Q^2_\nu, \end{aligned} \quad (8)$$

where

$$\begin{aligned} S^\dagger &= \sum_a \frac{\sqrt{2a+1}}{2}\left(C^\dagger_{\sigma a} \times C^\dagger_{\sigma a}\right)^0_0, \\ Q_\mu &= \sqrt{16\pi/5}\sum_{i=1}^{n} r_i^2 Y_{2\mu}(\theta_i \phi_i). \end{aligned} \quad (9)$$

By using the commutator, the D pair [42] can be obtained by

$$D^\dagger=\frac{1}{2}\left[Q^{(2)},S^\dagger\right]=\sum_{ab}y(ab2)(C_a^\dagger\times C_b^\dagger)^2. \quad (10)$$

The parameters G_σ and κ_σ are respectively the pairing interaction strength and quadrupole-quadrupole interaction strength between like-nucleons, while $\kappa_{\pi\nu}$ is the interactional strength of quadrupole-quadrupole interaction between protons and valence neutrons.

The E2 transition operator is

$$E2=\sum_{\sigma=\pi,\nu}e_\sigma Q_\sigma^2, \quad (11)$$

where e_π (e_ν) are effective charges of valence protons (neutrons), respectively. The M1 transition operator is

$$M1=\sum_{\sigma=\pi,\nu}M1(\sigma),$$
$$M1(\sigma)=g_l(\sigma)\hat{L}(\sigma)+g_s(\sigma)\hat{S}(\sigma), \quad (12)$$

where $g_l(\sigma)$ and $g_s(\sigma)$ are the orbital and spin g factors, which are fixed as those shown in Ref. [43], *i.e.*, $g_{l\pi}=1.1\ \mu_N^2$, $g_{l\nu}=-0.1\ \mu_N^2$, $g_{s\pi}=3.910\ \mu_N^2$, and $g_{s\nu}=-2.678\ \mu_N^2$.

3 Shape phase crossover

To see whether the SDPSM can produce the shape phase crossover and the similar shape phase transitional patterns obtained from the IBM, we study both identical nuclear system and neutron-proton coupled system in the SDPSM.

3.1 Vibration-γ-unstable transition

We begin by considering the vibration-γ-unstable phase, and choose a proton-neutron coupled system with valence nuclear pair $N_\pi=N_\nu=2$ in the 50∼82 shell. It should be noted that the valence protons are particle type, and the valence neutrons should be hole type in reproducing this (shape) phase crossover. The single-particle energies that we used are those shown in Refs. [21, 44] with the same values used in both the proton and neutron sectors, that is, 2.99, 2.69, 0.963, 0.0, 2.76 MeV for $j=s_{1/2},d_{3/2},d_{5/2},g_{7/2},h_{11/2}$ levels. The effective charges $e_\pi=1.5$e, $e_\nu=-0.5$e, where positive effective charge represents that of a real particle and the negative valued one represents that of the particle-hole one, that is the reason why the quadrupole-quadrupole interaction strength $\kappa_{\pi\nu}$ between valence protons and valence neutrons is negative in this paper. For simplicity, We set $G_\pi=G_\nu=G=0.28$ MeV, and $\kappa_\pi=\kappa_\nu=0$. From Fig. 1, one can see that energy ratio $R_{4_1}=E_{4_1}/E_{2_1}\sim2.0$ and the degenerate level structure of the vibrational states can be produced very well for $\kappa_{\pi\nu}\leqslant0.01$ MeV/r_0^4, such as $4_1^\dagger$, $2_3^\dagger$, $0_2^\dagger$, while $R_{4_1}=E_{4_1}/E_{2_1}\sim2.5$ and the level structure of the γ-unstable states can be reproduced for larger $\kappa_{\pi\nu}$ values.

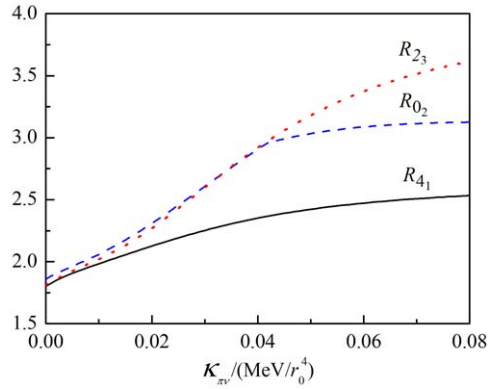

Fig. 1 (color online) Energy ratios R_{4_1}, R_{0_2} and R_{2_3} vs $\kappa_{\pi\nu}$ when $G=0.28$ MeV, $e_\pi=1.5$e, $e_\nu=-0.5$e, where energy ratio $R_{J_i}=E_{J_i}/E_{2_1}$.

The other energy ratios, $R_{6_10_2}=E_{6_1}/E_{0_2}$, $R_{6_10_3}=E_{6_1}/E_{0_3}$, $R_{0_2}=E_{0_2}/E_{2_1}$ and $R_{0_3}=E_{0_3}/E_{2_1}$ are presented in Fig. 2. For the fixed parameters, the results show that the level crossing-repulsion behavior indeed occurs in R_{0_2} and R_{0_3} within the critical region of the $U(5)$-$SO(6)$ transition[45]. In general, there is the crit-

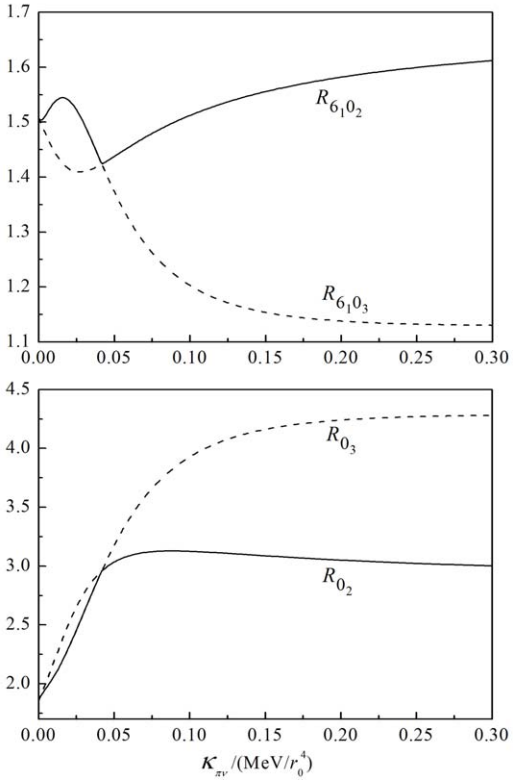

Fig. 2 The same as Fig. 1.

ical point of the $U(5)$-$SO(6)$ transition at which the level repulsion occurs, while the level crossing point is the critical point of the first order transition in the excited 0_2^+ and 0_3^+ states, which can be confirmed from electromagnetic transitions from these two states to the 2_1^+ or other low-lying states as discussed in the IBM[45].

The results for $B(\mathrm{E2};\ 0_2^+ \to 2_1^+)$, $B(\mathrm{E2};\ 0_3^+ \to 2_1^+)$ and $B(\mathrm{M1}; 0_1^+ \to 1_1^+)$, $B(\mathrm{M1}; 2_5^+ \to 2_1^+)$ are shown in Fig. 3. The left panel of Fig. 3 shows that a typical behavior of the crossing-repulsion when $\kappa_{\pi\nu} \sim 0.04$ MeV/r_0^4.

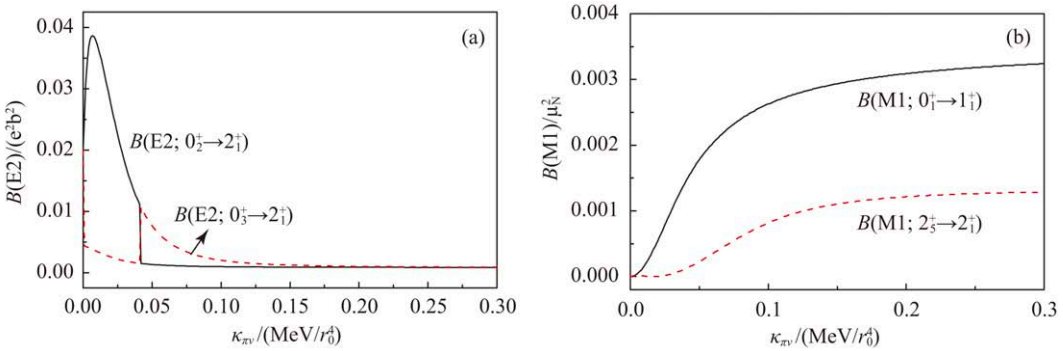

Fig. 3 (color online) $B(\mathrm{E2})$ values (a) and $BM1$ values (b) vs $\kappa_{\pi\nu}$ when $G = 0.28$ MeV, $e_\pi = 1.5$e, $e_\nu = -0.5$e.

Fig. 4 provides some energy ratios and $B(\mathrm{E2})$ values when $\kappa_{\pi\nu} = 0.01$ MeV/r_0^4. One can see from the left panel of Fig. 4 that $R_{4_1} = 2.5$ when $G = 0$ and $R_{4_1} = 2.0$ when G is lager than 0.2 MeV, where the degenerate level structure of the vibrational states ($U(5)$ symmetric states in the IBM) can be produced very well for larger G values. Hence, the γ-unstable and vibration spectra were produced. Interestingly, we also found that the crossing-repulsion behavior from the right panel of Fig. 4.

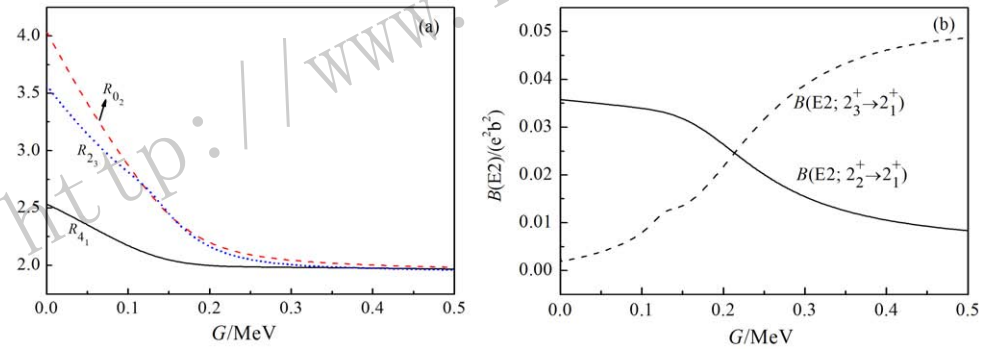

Fig. 4 (color online) Some energy ratios (a) and $B(\mathrm{E2})$ values (b) vs G when $\kappa_{\pi\nu} = 0.01$ MeV/r_0^4, $e_\pi = 1.5$e, $e_\nu = -0.5$e.

3.2 Vibration-rotation transitional patterns

The vibration-rotation transition is considered within a system of $N_\pi = N_\nu = 3$ in the gds shell[22]. We set $G_\pi = G_\nu = G$=0.2 MeV, $e_\pi = 3e_\upsilon$=1.5e. As an approximation, $\kappa_\pi = \kappa_\nu$ with the absolute value $\kappa_{\pi\nu} = 2\kappa_\sigma$. The single-particle energies that we used with the same values in both the proton and neutron sectors, that is, 2.99, 2.69, 0.963, 0.0, 0.0 MeV for $j = s_{1/2}, d_{3/2}, d_{5/2}, g_{7/2}, g_{9/2}$ levels[21]. From Fig. 5(a) one can see that the energy ratio $R_{4_1} = 2.0$ and the degenerate level structure of the vibrational states can be produced very well before $\kappa_\sigma \leqslant 0.0025$ MeV/r_0^4, while the level structure of the rotational states ($SU(3)$ symmetric states in the IBM) can be reproduced for larger κ_σ values. Although R_{4_1} is smaller than 2.0 when $\kappa_\sigma < 0.001$ MeV/r_0^4 and smaller than 3.33 when $\kappa_\sigma = 0.02$ MeV/r_0^4, the general behavior of the nuclear shape phase crossover from the vibrational to the rotational phase can be produced. Fig. 5(b) shows that the wiggling behavior of R_{4_1} from the vibrational to the rotational phase becomes obvious with the increasing of the number of the valence nucleon-pairs. The crossover behavior of $B(\mathrm{M1})$ is shown in Fig. 6. The reason why the energy ratio R_{4_1} are always smaller than the typical value for vibrational phase with 2.0 or rotational phase with 3.33 is due to the pauli-blocking effect, which plays an important role in producing the collectivity of the low-lying states. If proton-neutron coupled system is considered, the results will be close to the typical values of the limiting cases in the IBM.

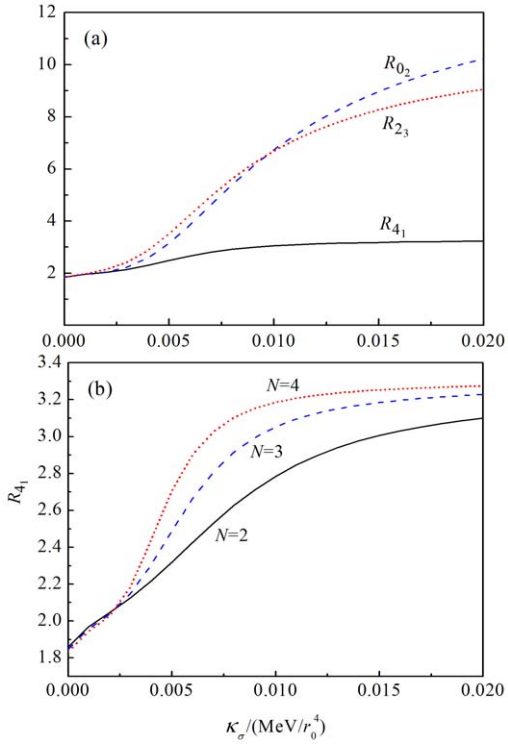

Fig. 5 (color online) Energy ratios when G_σ=0.2 MeV, $e_\pi = 3e_\upsilon = 1.5$e. (a) $R_{J_i} = E_{J_i}/E_{2_1}$ for $N_\pi = N_\nu = 3$, (b) R_{4_1} for $N_\pi = N_\nu = N = 2,3,4$.

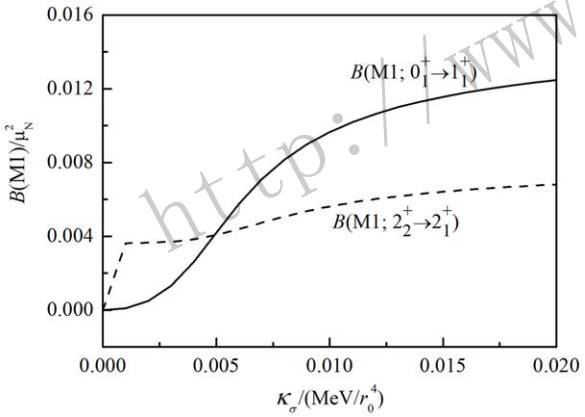

Fig. 6 B(M1) transitions vs κ_σ when $G_\sigma = 0.2$ MeV, $e_\pi = 3e_\upsilon = 1.5$e.

Fig. 7 provides energy ratio R_{4_1} and $B(M1)$ transitions when $\kappa_\sigma = 0.005$ MeV/r_0^4. One can see from Fig. 7(a) that the wiggling behavior of R_{4_1}, the typical feature of the phase transitional pattern between $SU(3)$ and $U(5)$, can be produced. It is shown that the rotational phase can be produced when $G = 0$, and then it changes quickly with G till $G = 0.2$ MeV, after that, it becomes saturate and close to the vibrational phase. The wiggling behavior of R_{4_1} from rotational to vibrational phase becomes obvious with the increasing of the number of valence nucleon-pairs. While the behavior of $B(M1)$ transitions shown in Fig. 7(b) with the variation of the control parameter is rather smooth.

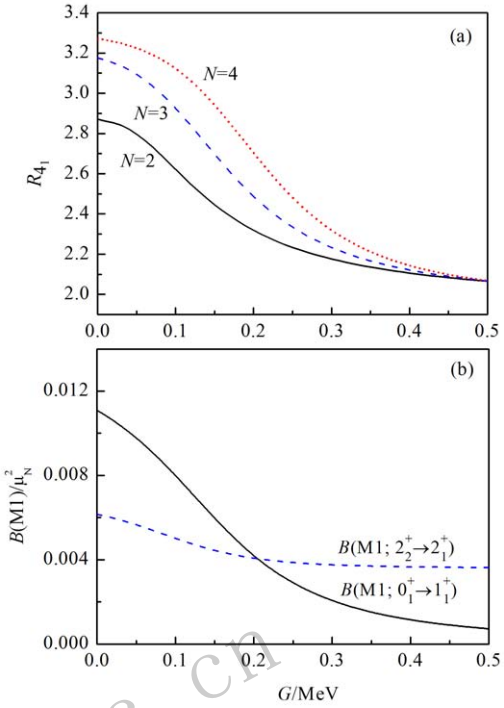

Fig. 7 (color online) Energy ratio R_{4_1} for $N_\pi = N_\nu = N$ =2,3,4 (a) and B(M1) transitions (b) vs G for $N_\pi = N_\nu = 3$, when κ_σ =0.005 MeV/r_0^4, $e_\pi = 3e_\upsilon$ =1.5e.

4 Summary

In summary, the nuclear shape phase crossover patterns are studied in the SD-pair shell model. Our results show that the shape phase transitional patterns shown in the IBM can also be produced in the SDPSM, though only crossover is observed due to the fact that the number of nucleon pairs is finite. With the increasing of the number of valence nucleon-pairs, the shape phase crossover will become more noticeable as demonstrated by the IBM calculations.

References:

[1] IACHELLO F, ARIMA A. The Interacting Boson Model[M]. Cambridge: Cambridge University Press, 1987.
[2] IACHELLO F, ZAMFIR N V, CASTEN R F. Phys Rev Lett, 1998, **81**: 1191.
[3] IACHELLO F. Phys Rev Lett, 2001, **87**: 052502.
[4] IACHELLO F, ZAMFIR N V. Phys Rev Lett, 2004, **92**: 212501.
[5] CASTEN R F, ZAMFIR N V. Phys Rev Lett, 2000, **85**: 3584.
[6] JOLIE J, CASTEN R C, BRENTANO P V, *et al*. Phys Rev Lett, 2001, **87**: 162501.
[7] GINOCCHIO J N, KIRSON M W. Phys Rev Lett, 1980, **44**: 1744.
[8] FENG D H, GILMORE R, DEANS S R. Phys Rev C, 1981, **23**: 1254.
[9] ISACKER P V, CHEN J Q. Phys Rev C, 1981, **24**: 684.

[10] JOLIE J, CEJNAR P, CASTEN R C, *et al*. Phys Rev Lett, 2002, **89**: 182502.
[11] WARNER D. Nature, 2002, **420**: 614.
[12] ROWE D J. Phys Rev Lett, 2004, **93**: 122502.
[13] ROWE D J, TURNER P S, ROSENSTELL G. Phys Rev Lett, 2004, **93**: 232502.
[14] CEJNAR P, HEINZE S, DOBEŠ J. Phys Rev C, 2005, **71**: 011304(R).
[15] LIU Y X, MU L Z, WEI H Q. Phys Lett B, 2006, **633**: 49.
[16] PAN F, DRAAYER J P, LUO Y A. Phys Lett B, 2003, **576**: 297.
[17] LEVIATAN A. Phys Rev Lett, 1996, **77**: 818; 2007, **98**: 242502; LEVIATAN A, ISACKER P V. Phys Rev Lett, 2002, **89**: 222501.
[18] ZHANG Y, HOU Z F, LIU Y X. Phys Rev C, 2007, **76**: 011305(R).
[19] ARIAS J M, GARCÍA-RAMOS J E, DUCKELSKY J. Phys Rev Lett, 2004, **93**: 212501 and the reference cited in this paper.
[20] CAPRIO M A, IACHELLO F. Phys Rev Lett, 2004, **93**: 242502.
[21] LUO Y A, PAN F, BAHRI C, *et al*. Phys Rev C, 2005, **71**: 044304.
[22] LUO Y A, ZHANG Y, MENG X F, *et al*. Phys Rev C, 2009, **80**: 014311.
[23] LUO Y A, PAN F, WANG T, *et al*. Phys Rev C, 2006, **73**: 044323.
[24] NIKŠIĆ T, VRETENAR D, LALAZISSIS G A, *et al*. Phys Rev Lett, 2007, **99**: 092502.
[25] LI Z P, NIKŠIĆ T, VRETENAR D, *et al*. Phys Rev C, 2009, **79**: 054301.
[26] ZHANG W M, FENG D H, GINOCCHIO J N. Phys Rev Lett, 1987, **59**: 2032.
[27] ZHANG W M, FENG D H, GINOCCHIO J N. Phys Rev C, 1988, **37**: 1281.
[28] ROWE D J, BAHRI C, WIJESUNDERA W. Phys Rev Lett, 1998, **80**: 4394.
[29] BAHRI C, ROWE D J, WIJESUNDERA W. Phys Rev C, 1998, **58**: 1539.
[30] GINOCCHIO J N. Phys Rev C, 2005, **71**: 064325.
[31] MCGRORY J B. Phys Rev Lett, 1978, **41**: 533.
[32] OTSUKA T. Nucl Phys, 1981, **368**: 244.
[33] HALSE P, JAQUA L, BARRETT B R. Phys Rev C, 1989, **40**: 968.
[34] CHEN J Q. Nucl Phys A, 1997, **626**: 686.
[35] CHEN J Q, LUO Y A. Nucl Phys A, 1998, **639**: 615.
[36] ZHAO Y M, YOSHINAGA N, YAMAJI S, *et al*. Phys Rev C, 2000, **62**: 014304.
[37] ALLAART K, BOEKER E, BONSIGNORI G, *et al*. Phys Rep, 1988, **169**: 209.
[38] HECHT K T, MCGRORY J B, DRAAYER J P. Nucl Phys A, 1972, **197**: 369.
[39] WU C L, FENG D H, CHEN X G, *et al*. Phys Rev C, 1987, **36**: 1157.
[40] LUO Y A, CHEN J Q, DRAAYER J P. Nucl Phys A, 2000, **669**: 101.
[41] DING X X, ZHANG Y, LI L, *et al*. Nucl Phys Rev, 2017, **34**: 98.
[42] TALMI I. Nucl Phys A, 1971, **172**: 1.
[43] LUO Y A, CHEN J Q, FENG T F, *et al*. Phys Rev C, 2001, **64**: 037303.
[44] FOGELBERG B, BLOMQVIST J. Nucl Phys A, 1984, **429**: 205.
[45] PAN F, WANG T, HUO Y S, *et al*. J Phys G: Nucl Part Phys, 2008, **35**: 125105.

SD配对壳模型对质量数$A\sim130$区原子核的形状渡越研究

丁小雪[1,1)]，罗延安[2]，何秉承[2]，潘 峰[1,3]，张 宇[1]，李 博[4]，J. P. Draayer[3]

（1. 辽宁师范大学物理系，辽宁 大连 116029；
2. 南开大学物理科学学院，天津 300071；
3. 美国路易斯安娜州立大学物理与天文系，LA 70803；
4. 鞍山师范学院物理科学与技术学院，辽宁 鞍山 114007）

摘要： 利用SD配对壳模型研究了质量数$A\sim130$区原子核的低激发态性质。为了减少参数，模型采用了等强度对力，取质子和中子对力强度等同近似，而非同类核子间的四极-四极相互作用强度取为同类核子间四极-四极相互作用强度的两倍。计算结果显示，模型的振动-转动和振动-γ不稳定运动的形状渡越特征与相互作用玻色子模型对应的形状相变特征基本吻合，从而说明SD配对壳模型是壳模型的一种合理近似。

关键词： SD配对壳模型；形状渡越；能级比；电磁跃迁

收稿日期：2018-09-11； **修改日期：**2018-11-13

基金项目：国家自然科学基金资助项目(11675071, 11747318, 11475091, 11875171)；美国国家科学基金项目(OIA-1738287, ACI-1713690)；美国能源部项目(DE-SC0005248)；中美奇特核理论研究所项目(CUSTIPEN)(DE-SC0009971)；LSU–LNNU 协作基金项目(9961)；鞍山师范学院科研启动基金资助项目(2018b03)

1) E-mail: wojiaodingxiaoxue@126.com。